

**Structure-property relations of low sintering
temperature scheelite-structured (1-x)BiVO₄-
xLaNbO₄ microwave dielectric ceramics**

Li-Xia Pang,^{a,c} Di Zhou,^{*b,c} Ze-Ming Qi,^d Wei-Guo Liu,^a Zhen-Xing Yue^c and Ian M.
Reaney^{*c}

^aMicro-optoelectronic Systems Laboratories, Xi'an Technological University, Xi'an
710032, Shaanxi, China

^bElectronic Materials Research Laboratory, Key Laboratory of the Ministry of
Education & International Center for Dielectric Research, Xi'an Jiaotong University,
Xi'an 710049, Shaanxi, China

^cMaterials Science and Engineering, University of Sheffield, Sheffield, S1 3JD, UK

^dNational Synchrotron Radiation Laboratory, University of Science and Technology
of China, Anhui, 230029, Hefei, China

^eState Key Laboratory of New Ceramics and Fine Processing, Department of
Materials Science and Engineering, Tsinghua University, Beijing 100084, China

*Corresponding author. Tel: +86-29-82668679; Fax: +86-29-82668794; E-mail address: zhoudi1220@gmail.com
(Di Zhou) & i.m.reaney@sheffield.ac.uk (Ian M. Reaney)

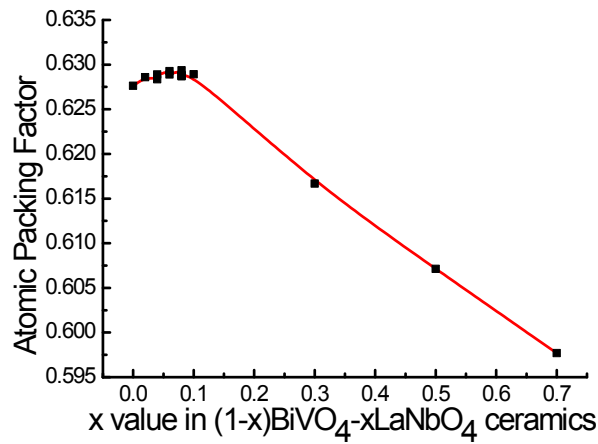


Fig. S1 Atomic packing factor of the $(1-x)\text{BiVO}_4-x\text{LaNbO}_4$ ($0.0 \leq x \leq 0.7$) ceramics as a function of x value

Atomic packing factors of the $(1-x)\text{BiVO}_4-x\text{LaNbO}_4$ ($0.0 \leq x \leq 0.7$) ceramics as a function of x value are shown in Fig. S1. It is noticed that in the $(1-x)\text{BiVO}_4-x\text{LaNbO}_4$ ($0.0 \leq x \leq 0.7$) ceramics, the A-site is 8-fold coordinated, and the Bi^{3+} and La^+ cations have a radius of 1.17\AA and 1.16\AA , respectively. On the B-site which is 4-fold coordinated V^{5+} and Nb^{5+} cations have a radius of 0.355\AA and 0.48\AA , respectively, according to Shannon's data set. The equivalent ionic radius on B site increase with x value much faster than the decrease in ionic radius on A site, which resulted in a linear increase in equivalent atom volume. It is understandable that the cell volume increases with x value in the tetragonal phase region. However, in the monoclinic phase region, the cell volume decreases slightly with the x value and reaches a minimum at about $x=0.1$. Combined with the equivalent atom volume and cell volume trend, a maximum value of atomic packing factor can be achieved at about $x=0.1$ as shown in Fig. S1. Atomic packing factor increased slightly as x value increased and reached a peak at about $x=0.1$. Then it decreased linearly with x value within the scheelite phase region. The substitution of Nb^{5+} for V^{5+} on the B site dominated the increase in atomic packing factor and gave much internal pressure to

the monoclinic scheelite structure and lead the transition from monoclinic to tetragonal structure. In the monoclinic phase region, the atomic packing factor reached a maximum value of about 62.9 % at $x = 0.08$ and 0.10 .

As seen from the phonon parameters listed in the tables (S1, S2 and S3) below, the dielectric polarization contribution from the vibration modes below 150 cm^{-1} can reach above 85 % of the total value for $x = 0.02, 0.06, 0.08,$ and 0.10 sample, and it is quite different from low permittivity materials, such as Ag_2MoO_4 and NaAgMoO_4 . This implies that the dielectric polarization contribution of monoclinic scheelite solid solution mainly comes from external modes, i.e. the vibrational modes of Bi-O stretching. However, due to the overlapping of modes at low wave number, the accuracy of the calculated ϵ_r was influenced by errors from fitting. The neighboring structure of Bi^{3+} accounts for the change of macroscopical permittivity due to its large polarizability (6.12 \AA^3) which is greater than that of the V^{5+} ion (2.92 \AA^3). Hence, although the overlapping of $\delta_{as}(\text{VO}_4)$ mode and the $\delta_s(\text{VO}_4)$ corresponding to the ferroelastic phase transition can be observed in Raman and IR spectra, their contribution to the microwave ϵ_r was low, and their influence ignored.

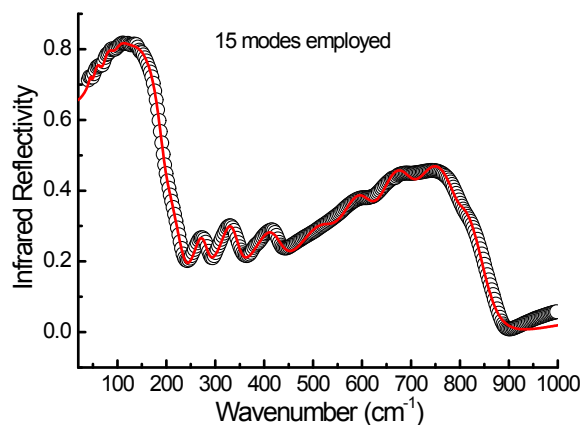


Fig. S2 Measured and calculated infrared reflectivity spectra of $x = 0.10$ ceramic (solid line for fitting values and circle for measured values) using 15 modes

Besides, for the $x = 0.10$ sample, both the monoclinic and tetragonal models were employed to do the fitting. The measured and calculated infrared reflectivity spectra of $x = 0.10$ ceramic (solid line for fitting values and circle for measured values) using 15 modes (be treated as tetragonal phase) are shown in Fig. S2. Compared with the result in Fig. 5(a), there is no macroscopic difference. Both the monoclinic and tetragonal models fitting work well. For monoclinic model, a sum of 16 modes were used to fit the IR spectra and there were two modes at 321.61 and 335.56 cm^{-1} , respectively, observed according to the bending of tetrahedron. For tetragonal model, 15 modes were used to fit and there was only one mode at 330.07 cm^{-1} for the bending mode of tetrahedron. There contribution to the dielectric permittivity can be found in Table S4 and S5, and only negligible difference was observed.

Table S1. Phonon parameters obtained from the fitting of the infrared reflectivity spectra of x=0.02 ceramic

Mode	ω_{oj}	ω_{pj}	γ_j	$\Delta\epsilon_j$
1	63.611	278.76	16.509	19.2
2	77.995	437.77	15.508	31.5
3	101.32	352.57	22.94	12.1
4	129.55	103.34	15.535	0.636
5	144.15	97.094	11.94	0.454
6	201.95	119.14	31.342	0.348
7	233.67	138.56	48.539	0.352
8	278.31	171.99	28.318	0.382
9	315.87	166.43	31.051	0.278
10	353.05	222.53	30.517	0.397
11	411.16	273.72	55.063	0.443
12	490.25	450.18	99.578	0.843
13	575.75	554.26	83.965	0.927
14	636.32	578.97	78.373	0.828
15	706.53	363.17	84.643	0.264
16	799.47	133.46	43.337	0.0279
x=0.02	$\epsilon_\infty=3.91$		$\epsilon_0=72.95$	

Table S2. Phonon parameters obtained from the fitting of the infrared reflectivity spectra of x=0.06 ceramic

Mode	ω_{oj}	ω_{pj}	γ_j	$\Delta\epsilon_j$
1	61.658	263.94	15.847	18.3
2	74.922	347.2	16.549	21.5
3	86.215	309.68	18.872	12.9
4	102.04	345.31	28.563	11.5
5	133.87	198.98	39.807	2.21
6	204.36	117.1	41.118	0.328
7	224.27	108.65	49.717	0.235
8	272.95	195.82	37.005	0.515
9	322.49	182.81	31.697	0.321
10	344.02	193.18	37.937	0.315
11	414.01	357.3	68.565	0.745
12	517.52	467.37	93.744	0.816
13	591.88	580.59	74.025	0.962
14	653.56	599.81	72.11	0.842
15	720.3	372.92	78.481	0.268
16	803.1	112.35	43.257	0.0196
x=0.06	$\epsilon_\infty=4.33$		$\epsilon_0=76.06$	

Table S3. Phonon parameters obtained from the fitting of the infrared reflectivity spectra of x=0.08 ceramic

Mode	ω_{oj}	ω_{pj}	γ_j	$\Delta\epsilon_j$
1	46.388	113.34	8.7132	5.97
2	59.572	303.84	19.434	26
3	76.166	427.63	26.082	31.5
4	97.298	261.28	34.984	7.21
5	136.29	146.72	51.37	1.16
6	200.75	116.31	40.566	0.336
7	219.39	112.49	57.389	0.263
8	275.83	188.92	38.436	0.469
9	321.89	137.17	30.211	0.182
10	336.76	213.93	44.993	0.404
11	411.18	346.88	70.949	0.712
12	507.71	434.27	99.032	0.732
13	580.77	491.55	86.228	0.716
14	649.35	461.55	85.614	0.505
15	723.21	290.27	86.656	0.161
16	799.61	103.01	54.4	0.0166
x=0.08	$\epsilon_\infty=3.22$	$\epsilon_0=79.6$		

Table S4. Phonon parameters obtained from the fitting of the infrared reflectivity spectra of x=0.10 ceramic as monoclinic phase using 16 modes

Mode	ω_{oj}	ω_{pj}	γ_j	$\Delta\epsilon_j$
1	46.401	88.514	5.9579	3.64
2	60.248	300.65	17.176	24.9
3	77.761	440.85	24.285	32.1
4	97.516	329.34	32.591	11.4
5	123.92	218.24	57.642	3.1
6	205.74	107.5	43.363	0.273
7	223.55	93.022	47.995	0.173
8	271.38	198.12	38.935	0.533
9	321.61	150.02	31.11	0.218
10	335.56	212.84	39.44	0.402
11	413.37	367.62	69.807	0.791
12	516.38	447.48	89.404	0.751
13	585.82	563.68	76.096	0.926
14	653.24	559.66	75.551	0.734
15	721.34	358.14	79.441	0.247
16	801.28	108.67	50.891	0.0184
x=0.10	$\epsilon_\infty=4.03$		$\epsilon_0=84.28$	

Table S5. Phonon parameters obtained from the fitting of the infrared reflectivity spectra of x=0.10 ceramic as tetragonal phase using 15 modes

Mode	ω_{oj}	ω_{pj}	γ_j	$\Delta\epsilon_j$
1	46.217	88.275	5.843	3.65
2	60.22	302.64	17.397	25.3
3	77.785	440.92	24.365	32.1
4	97.57	328.17	32.555	11.3
5	124	216.95	57.234	3.06
6	206.72	113.38	44.576	0.301
7	225.74	89.724	50.141	0.158
8	271.01	189.57	36.904	0.489
9	330.07	272.02	43.55	0.679
10	413.6	362.64	68.645	0.769
11	516.17	447.6	89.527	0.752
12	585.77	564.18	76.179	0.928
13	653.23	559.59	75.541	0.734
14	721.33	358.07	79.406	0.246
15	801.26	108.69	50.922	0.0184
x=0.10	$\epsilon_{\infty}=4.03$		$\epsilon_0=84.51$	